mation are quite small. Although the magnitude of the binding energy varies when a larger basis set is employed and electron correlation effects are included, the qualitative trends for the series under study remain essentially unchanged. At all levels of calculation, the relative affinity of the hydrogen donors for benzene is found to be HF > H_2O, HCl > H_2S, NH_3. Where comparison is possible, the results of the calculations appear to be in fair agreement with experimental findings. The theoretical distances from the halide atoms to the ring center are slightly longer than the values obtained from analysis of the rotational spectra. According to both experiment and theory, the dipole moment of C_6H_6···HF is substantially larger than that of HF. Since the theoretical calculations predict similar dipole moment enhancements for all dimers, the benzene ring seems to act as an electron donor in these systems.

Although this work has been concentrated on a limited domain of complex geometries, the results suggest that further use of this theoretical approach may be fruitful for exploring other configurations of the C_6H_6···AH_n systems. It is of particular interest to determine whether the theory predicts other structures to be more favorable than those involving π hydrogen bonding. Investigations undertaken to answer this question will be the subject of a future report.

Acknowledgment. This work was carried out on the Cray 1S computer at the University of London Computer Centre. We thank Drs. R. D. Amos and N. C. Handy for helpful discussions on the use of CADPAC.

Registry No. C_6H_6, 71-43-2; HF, 7664-39-3; HCl, 7647-01-0; H_2O, 7732-18-5; H_2S, 7783-06-4; NH_3, 7664-41-7.

Molecular Dynamics Simulation of Interfacial Water Structure and Dynamics in a Parvalbumin Solution

Peter Ahlström,* Olle Teleman, and Bo Jönsson

Contribution from Physical Chemistry 2, Chemical Centre, University of Lund, P.O.B. 124, S-221 00 Lund, Sweden. *Received October 28, 1987*

Abstract: A 106-ps molecular dynamics simulation of the calcium-binding protein parvalbumin in water has been used as a basis for studying interfacial water. A general conclusion is that structure and dynamics of the interfacial water are only marginally affected by the presence of the protein. A few water molecules, which reside close to charge groups, are immobilized throughout the simulation. In the analysis the water molecules have been classified according to the distance to the nearest protein atom. Close to the protein we find a decrease in radial diffusion, while lateral diffusion is enhanced. In the inner water layers the dipole moment vector is preferentially oriented perpendicular to the radius vector of the protein. The reorientational correlation times have a minimum 4–5 Å from the protein, with values similar to those obtained from simulations of pure water.

It is commonly believed that a foreign body in a water solution imposes some ("clathrate-like" or icelike) structure on the water, in order to minimize the number of nonfulfilled hydrogen bonds. This applies especially to hydrophobic bodies since they are unable to form any hydrogen bonds at all but also to nonionic hydrophilic ones since they do not normally form hydrogen bonds as easily as water. Such a structure would, of course, affect the dynamics near the surface.

Experimental Results. The structure and dynamic behavior of a solvent close to a surface have received considerable attention. In particular, the influence of biological macromolecules on water structure and dynamics has been the subject of several experimental studies with varying methods, among others infrared spectroscopy,[1] Mössbauer and microwave spectroscopy,[2] and nuclear magnetic resonance. Koenig et al.[3] studied interfacial water in protein solutions by means of ^2H and ^1H NMR relaxation measurements. However, as was pointed out by Piculell and Halle,[4] ionizable groups at the protein contribute considerably to deuteron and proton relaxation rates, which are thus unsuitable for studies of interfacial water. Instead, the latter authors used ^{17}O relaxation data to obtain information about water dynamics around several proteins, among these carp parvalbumin.[5] They found that the local water reorientation at the protein surface was anisotropic and could be characterized by two relaxation times. They concluded that approximately two water layers close to the protein were affected by the surface with significantly reduced reorientational dynamics as compared to bulk water. On assumption of time-scale separation, they also concluded that the local rapid motion at the protein surface, which by necessity is anisotropic, is followed by a much slower reorientation with a correlation time in the nanosecond region. Another approach was made by Polnaszek and Bryant,[6] who studied proton relaxation of interfacial water using a spin label bound to a protein surface. They found a 5–10-fold decrease in the translational diffusion near (<10 Å) the protein surface.

In another study[7] of water in silica sols, Halle and Piculell found qualitatively the same behavior. For this system they also applied a dynamic model in order to interpret the long correlation time. Their conclusion[8] was that the translational mobility of the hydration water is strongly reduced; the radial diffusion is decreased by 2 orders of magnitude, and the lateral diffusion is decreased by 1 order of magnitude compared to bulk water.

Simulations of Water at Surfaces. Both Monte Carlo (MC) and molecular dynamics (MD) simulations are well suited to study water at interfaces. Preferentially, a simplified model system is

(1) Poole, P. L.; Finney, J. L. In *Biophysics of Water*; Franks, F., Mathias, S., Eds.; Wiley-Interscience: Chichester, U.K., 1982; p 36.
(2) Parak, F. *Methods Enzymol.* **1986**, *127*, 196.
(3) Koenig, S. H.; Hallenga, K.; Sphorer, M. *Proc. Natl. Acad. Sci. U.S.A.* **1975**, *72*, 2667.
(4) Piculell, L.; Halle, B. *J. Chem. Soc., Faraday Trans. 1* **1986**, *82*, 401.
(5) Halle, B.; Andersson, T.; Forsên, S.; Lindman, B. *J. Am. Chem. Soc.* **1981**, *103*, 500.
(6) Polnaszek, C. F.; Bryant, R. G. *J. Chem. Phys.* **1984**, *81*, 4038.
(7) Piculell, L. *J. Chem. Soc., Faraday Trans. 1* **1986**, *82*, 387.
(8) Halle, B.; Piculell, L. *J. Chem. Soc., Faraday Trans. 1* **1986**, *82*, 415.

0002-7863/88/1510-4198$01.50/0

employed, where the effects of only a few parameters are studied, for example, water between two planar surfaces. The surfaces can be modeled by purely repulsive walls as in the simulation of MCY[9] water by Jönsson[10] or as consisting of fixed atoms interacting with the waters via a Lennard–Jones-type potential. Recently, a short review was presented by Parsonage.[11] In most simulations the water next to the surface is preferentially oriented with its dipole vector parallel to the surface. Lee et al.[12] (MD simulation of the ST2[13] water model) and Valleau and Gardner[14] (MC simulation of the TIPS2[15] water model) found that the interfacial water structure resembles that of ice-I with one hydrogen directed toward the surface. However, Valleau and Gardner reported severe convergence problems for their MC calculations and therefore made their simulation at an enhanced temperature, 399 K, i.e. above the boiling point of real water.

Sonnenschein and Heinzinger[16] made an MD simulation of ST2 water near a Lennard–Jones surface from which they reported a slight increase (about 30%) of the diffusion coefficient for the water next to the surface. They claimed that it was due to fewer hydrogen bonds in the interfacial layer. Others found, however, a slight decrease of the diffusion for ST2[17] as well as for MCY[18] water and also some anisotropy in the diffusion coefficient. Barabino et al.[18] also reported prolonged correlation times (about 50%) for water reorientation near "hard" walls but not near "soft" (Lennard–Jones etc.) walls.

Until recently, there existed only a few simulations of large particles in solution. In 1979 Rossky and Karplus[19] made a short (1.5-ps) MD simulation of a dipeptide in ST2 water. The rotational correlation times increased by a factor of 3 for the first layer of water next to the hydrophobic parts of the amino acids whereas the water next to hydrophilic parts of the peptide was much less affected (correlation times increased by about 50%). A MD study of a repulsive cavity in an SPC[20] water bath was made by Postma et al.[21] They found that for a cavity with radius 3 Å two water orientations seem to be preferred, either with one O–H vector directed outward from the cavity or with the water molecule bisected by the radius vector with the hydrogens turned toward the cavity. The radical diffusion was obtained approximately from "residence time distributions" (corresponding to the propagators described below) for different water layers around the cavity. The diffusion coefficients obtained were 8×10^{-9}, 6×10^{-9}, and 5×10^{-9} m^2/s for the first (thickness 1.75 Å), second (2,85 Å), and third (1,4 Å) hydration shell, respectively, i.e. increasing diffusion near the cavity. However, these values do not differ very much from the bulk value from the same simulation (6.8×10^{-9} m^2/s).

A study of the effect of two spheres in ST2[13] water was made by Zichy and Rossky.[22] The two spheres, corresponding to krypton atoms, were placed at a center to center distance of 7.13 Å. The two spheres decreased the diffusion coefficient about 30%, compared to the bulk, for water molecules starting within 5 Å from either of the two spheres. They also found that hydrogen bonds were stabilized near the spheres and that rotational correlation times were increased about 30% in the 5-Å shell.

Few authors have reported results for water in simulations of biological macromolecules. Berendsen et al. made a 40-ps simulation of a hydrate crystal of pancreatic trypsin inhibitor (PTI)[23] containing 4 PTI molecules (of 58 amino acids each), 552 SPC water molecules, and 24 Cl^- as counterions. They calculated the root-mean-square fluctuation for the water positions during 30 ps and found that most of them were less than 2.5 Å and that the highest rms fluctuation was less than 6 Å compared to 8 Å obtained from bulk diffusion. They concluded that waters remained about 10 ps in the ordered water positions found in the X-ray structure. Wong and McCammon simulated trypsin in a solution of SPC water[24] and found the diffusion coefficients to vary from 1.6×10^{-9} to 5×10^{-9} m^2/s for water molecules starting at 3–15 Å from the protein surface, respectively. This is to be compared to 3.6×10^{-9} m^2/s from a bulk simulation of rigid SPC water.

To study the effects of the interaction between water and macromolecules, we made a simulation of the calcium-binding protein parvalbumin in aqueous solution. In an earlier paper,[25] we showed the influence of water on protein structure and dynamics, and in this study, we will focus on the influence of the protein molecule on the surrounding water.

Methods

The trajectory from a simulation of parvalbumin (M_r 11 471 g/mol) in water[25] was used in this study. Parvalbumin has two calcium-binding sites consisting of carboxylic groups and carbonyl oxygens from peptide bonds. In the X-ray structure (denoted F6-A) as determined by Kretsinger and Nockolds,[26] one of the calcium ions coordinates one water molecule as well. The protein consists of 108 amino acids, which form six α-helices (denoted A–F) connected by short loops. The calcium-binding sites are situated between helices C and D and between E and F. The protein contains a large amount (about one-third) of charged amino acids and has a net charge of −7 without calcium ions.

Interaction Potential. The interaction potential has been discussed in detail elsewhere.[27] It is based on inter- and intramolecular site–site interactions between atoms and groups of atoms (pseudoatoms). All atoms are described explicitly except hydrogens in CH, CH_2, and CH_3 groups, which are treated as pseudoatoms. The potential function between two sites is decomposed into two parts, namely covalent and noncovalent interactions. The latter act between atoms in different molecules and between atoms in the same molecule that are separated by more than two bonds. The noncovalent potential between two sites i and j is described by eq 1 where ϵ_{ij} and σ_{ij} are the usual Lennard–Jones parameters

$$U_{ij}(r) = 4\epsilon_{ij}[(\sigma_{ij}/r)^{12} - (\sigma_{ij}/r)^6] + q_iq_j/4\pi\epsilon_0\epsilon_r r_{ij} \quad (1)$$

and q_i is the charge on site i. The parameters were taken from the literature,[20,28-30] and we used the Kirkwood–Slater[30] formula to calculate the LJ coefficients with the assumption that the LJ potential minimum corresponds to the sum of the van der Waals radii of the two atoms. The dielectric permittivity was set equal to unity.

All internal bond and bond angle vibrations were treated explicitly, and the potential functions are given by eq 2 where x_i and $x_{i,eq}$ are the

$$U_{intra} = \sum_{bonds}[K_b(x_i - x_{i,eq})^2/2] + \sum_{angles}[K_a(\theta_i - \theta_{i,eq})^2/2] \quad (2)$$

actual bond length and equilibrium distance, respectively, with similar notation for angles. Here, we have assumed harmonicity and taken the force constants K_a and K_b from the literature.[20,28,29,31,32] The interactions

(9) Matsuoka, O.; Clementi, E.; Yoshimine, M. *J. Chem. Phys.* **1976**, *64*, 1351.
(10) Jönsson, B. *Chem. Phys. Lett.* **1981**, *82*, 520.
(11) Parsonage, N. G. In *Trends in Interfacial Electrochemistry*; Silva, A. F., Ed.; Reidel: Dordrecht, The Netherlands, 1986; p 359.
(12) Lee, C. Y.; McCammon, J. A.; Rossky, P. J. *J. Chem. Phys.* **1984**, *80*, 4448.
(13) Stillinger, F. H.; Rahman, A. *J. Chem. Phys.* **1974**, *60*, 1545.
(14) Valleau, J. P.; Gardner, A. A. *J. Chem. Phys.* **1987**, *86*, 4162.
(15) Jorgensen, W. L. *J. Chem. Phys.* **1982**, *60*, 4156.
(16) Sonnenschein, R.; Heinzinger, K. *Chem. Phys. Lett.* **1983**, *102*, 550.
(17) Marchesi, M. *Chem. Phys. Lett.* **1983**, *97*, 224.
(18) Barabino, G.; Gavotti, C.; Marchesi, M. *Chem. Phys. Lett.* **1984**, *104*, 478.
(19) Rossky, P.; Karplus, M. *J. Am. Chem. Soc.* **1979**, *101*, 1913.
(20) Berendsen, H. J. C.; Postma, J. P. M.; van Gunsteren, W. F.; Hermans, J. In *Intermolecular Forces*; Pullman, B., Ed.; Reidel: Dordrecht, The Netherlands, 1981; p 331.
(21) Postma, J. P. M.; Berendsen, H. J. C.; Haak, J. R. *Faraday Symp. Chem. Soc.* **1982**, *17*, 55.
(22) Zichy, D. A.; Rossky, P. J. *J. Chem. Phys.* **1986**, *84*, 2814.
(23) Berendsen, H. J. C.; van Gunsteren, W. F.; Zwinderman, H. R. J.; Geurtsen, R. G. *Ann. N.Y. Acad. Sci.* **1986**, *482*, 269.
(24) Wong, C. F.; McCammon, J. A. *Isr. J. Chem.* **1986**, *27*, 211.
(25) Ahlström, P.; Teleman, O.; Jönsson, B.; Forsén, S. *J. Am. Chem. Soc.* **1987**, *109*, 1541.
(26) Kretsinger, R. H.; Nockolds, C. E. *J. Biol. Chem.* **1973**, *218*, 3313.
(27) See ref 25 and its supplementary material with corrections.
(28) Hermans, J.; Berendsen, H. J. C.; van Gunsteren, W. F.; Postma, J. P. M. *Biopolymers* **1984**, *23*, 1513.
(29) van Gunsteren, W. F.; Karplus, M. *Macromolecules* **1982**, *15*, 1528.
(30) Margenau, M.; Kestner, N. R. *Theory of Intermolecular Forces*; Pergamon: New York, 1969.
(31) Dolphin, D.; Wick, A. E. *Tabulation of Infrared Spectral Data*; Wiley-Interscience: New York, 1977.
(32) Herzberg, G. *Molecular Spectra and Molecular Structure: Infrared and Raman Spectra of Polyatomic Molecules*; Van Nostrand: Princeton, NJ, 1945.

Table I. Simulation Parameters and Averages

no. of atoms	7970
box size, Å	43 × 50 × 43
time step $\Delta t/\Delta T$, fs	0.2/1.2
equilibration time, ps	36
length of trajectory, ps	70
velocity scaling interval, fs	99.6
av scaling factor	0.98
neighbor list update interval, fs	4.8
av temp, K	303

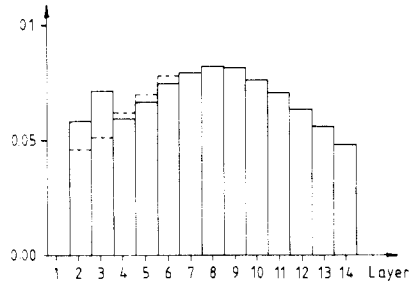

Figure 1. Mean fractions of water molecules in different shells (solid curve) compared to the fractions calculated assuming the shells to be 1-Å-thick spherical shells with radius equal to its r_G (broken curve).

due to internal rotation in the protein were handled by means of periodic dihedral potentials (eq 3). Ψ_k is a dihedral angle and $C_{k,n}$ an interaction parameter; k runs over all dihedral angles at each bond. The parameters used in eq 1–3 are given in the supplementary material mentioned in ref 27.

$$U_{\text{int rot}} = \sum_k \sum_{n=1}^{3} C_{k,n}[1 - \cos(n\Psi_k)] \quad (3)$$

For the water–water interactions a modification[33] of the empirical simple point charge (SPC) model by Berensen et al.[20] allowing for internal flexibility was used. The main reason for this choice was simplicity as the SPC model conforms to the interaction expression (eq 1). Unfortunately, there has, as far as we know, not yet been any determination of the dielectric permittivity for SPC water. A simulation[34] for the nonempirical so-called MCY water potential[9] gives a dielectric permittivity of about 35, and there is no obvious reason for the SPC model to be more accurate. A discussion of modeling internal flexibility is found in ref 33.

Simulation Procedure. The molecular dynamics program used, MUMOD,[35] uses a double-time step Gear[36] algorithm. Bond length and bond angle coordinates were integrated with a time step $\Delta t = 0.2$ fs (fs = 10^{-15} s) whereas, for more slowly varying degrees of freedom, a time step $\Delta T = 1.2$ fs was used.

The protein (in its X-ray configuration) was placed at the center of the simulation box together with the 23 crystal waters. The box was then filled with 2307 water molecules placed on the bases of a primitive cubic lattice to give the correct density and a protein concentration of about 18 mM. Three randomly chosen waters were exchanged for sodium ions to make the system electroneutral. The simulation was performed with periodic boundary conditions in all directions and a spherical cutoff for interactions using a neighbor list technique. The cutoff radius for all atoms in a water molecule was calculated from the oxygen of that molecule to avoid artifacts arising from a split dipole. Simulation parameters are given in Table I.

Results

In the analysis, water molecules were classified at each moment according to the distance d between the water oxygen and the nearest protein atom. The classes were numbered as the integer part of the distance in angstroms for water molecules with $d <$ 15 Å. Class 15 comprised the remaining water molecules. The fraction of molecules in each class, averaged over the whole analysis period, is shown in Figure 1 and Table II. The numbers

(33) Teleman, O.; Jönsson, B.; Engström, S. *Mol. Phys.* **1987**, *60*, 193.
(34) Neumann, M. *J. Chem. Phys.* **1985**, *82*, 5663.
(35) Teleman, O.; Jönsson, B. *J. Comput. Chem.* **1986**, *7*, 58.
(36) Gear, C. W. *Numerical Initial Value Problems in Ordinary Differential Equations*; Prentice-Hall: Englewood Cliffs, NJ, 1971; p 148.

Table II. Classification of Water Molecules and Their Fractions of All Water in the Different Layers and Corresponding Radii of Gyration[a]

class	d_s/Å	mean fraction	r_G/Å	ideal fraction
1	1–2	6×10^{-5}		
2	2–3	0.058	15.8–16.7	0.045–0.050
3	3–4	0.071	16.6–17.6	0.050–0.055
4	4–5	0.059	18.1–19.1	0.061–0.064
5	5–6	0.066	19.4–20.3	0.068–0.074
6	6–7	0.075	20.4–21.3	0.075–0.082

[a] The last column is calculated assuming ideal spherical shells with radius r_G and thickness 1 Å (water volume assumed to be 30 Å^3/molecule and a total of 2327 water). The radii of gyration varied through the simulation, and therefore an interval is given. The shells after class 6 were incomplete and thus a comparison with the idea is irrelevant.

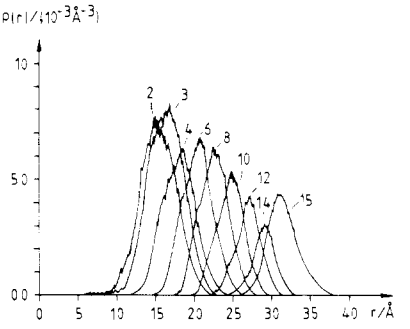

Figure 2. Radial distribution of water atoms around the center of mass of the protein for different classes.

from class 8 and upward decrease as the layers from and including layer 6 are not fully contained within the minimum image. As can be seen from Figure 1, there occurs a maximum in class 3. There are two reasons for this effect: packing and roughness of the protein.

Since the water has a van der Waals radius of 1.78 Å and most heavy atoms in the protein have about the same van der Waals radius, a maximum in the radial distribution function at ≈3.5 Å is expected. The waters in class 2 thus have mostly hydrogen atoms as their next protein atom. The maximum in layer 3 is followed by a distribution minimum in layer 4.

The radius of gyration of a water layer was obtained as eq 4 where r_i is the distance between atom i and the center of mass for the layer. The radii of gyration are given in Table II. We

$$r_G^2 = \sum_{\text{layer}} m_i r_i^2 / \sum m_i \quad (4)$$

note that r_G increases by about 1 Å on going from one layer to the next, except between layers 3 and 4 where the step is 1.5 Å. Thus, layer 3 had creases or wrinkles too small for layer 4 to follow; that is, the roughness of the protein is of the order of 4–6 Å in size (which is apparent also from visual inspection). If one assumes the protein to be a uniform sphere, the outer radius of the protein can be obtained as $0.6^{-0.5} r_G$ where r_G is its radius of gyration. In the simulation $r_G = 12.0$ Å for the protein corresponding to a sphere of radius 15.5 Å as compared to 15.8–16.7 Å for the innermost water layer. The difference between these two radii is much smaller than the minimum distance between a water molecule and a protein atom, which also indicates that the inner water layer followed a rough protein surface. See also Figure 2, which shows the radial distribution of water around the protein center of mass for some classes of water. We have compared the actual layer populations to those of spherical layers with radius r_G in bulk water (see Figure 1). The considerable surplus in layers 2 and 3 again indicates that these layers followed the protein surface whereas layer 4 was smoother.

The mean residence time for water molecules in a given shell was for the innermost layer (number 2) nearly 1 ps, while much shorter in all other layers. (In bulk water, the mean-square displacement over a half-layer thickness takes of the order of 0.2 ps with a diffusion coefficient of 6.1×10^{-9} m^2/s.) This was due

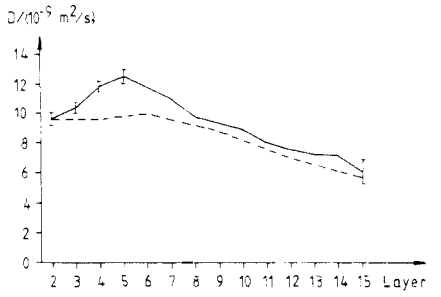

Figure 3. Diffusion coefficient for water molecules as a function of the starting class: dashed curve, followed 20 ps; solid curve, followed 1.0 ps. The error bars were obtained from a standard statistical analysis based on subtrajectories 10 ps long.

to water diffusion as well as protein fluctuations. The short lifetimes made it difficult to unequivocally assign a given water molecule to a single class. To choose only waters that stayed in the same class during the period required for a certain analysis would have biased results because of the preference for immobile water molecules. We chose the following model: Suppose that a certain analysis required water molecules to be followed for at least a time ϑ. All water molecules in the observed layer at time $t = t'$ were included in the analysis, irrespective of their remaining in the layer or leaving it before $t = t' + \vartheta$. Unfortunately, this led to some mixing of results for different layers, especially for properties averaged over longer periods. Since the diffusion coefficient for water molecules was $\approx 8 \times 10^{-9}$ m^2/s on average (see below), the root-mean-square displacement in 10 ps was ≈ 7 Å. Thus, properties that were calculated over such a long time were averaged over a few neighboring classes. The contribution of each water molecule to evaluated properties was weighted by $w + \vartheta$, where w is the actual residence time of that water molecule in the observed layer.

Bound Waters. As a start for the search for water-binding sites, we determined the accumulated time when the distance between a given water molecule and a given protein atom was less than 4 Å. This time was just a few picoseconds with a few exceptions. So the waters that liganded the calcium ions did stay there for the whole analysis period, except for the original crystal water, which left 10 ps after the equilibration. This shows that the residence time for a water molecule liganded to Ca^{2+} is longer or much longer than 70 ps, which seems to be in agreement with experimental results for the aquo calcium complex. Some water molecules resided near charged groups or ion pairs for tens of picoseconds. One example is a water molecule that remained close to the ion pair formed by Lys-71 and Glu-16 during most of the simulation. Other examples are the water molecules that formed hydrogen bonds to charged protein atoms. Among these were the ones that formed alternating hydrogen bonds to the two O^{δ} atoms of Asp-42, the water that formed shifting hydrogen bonds to the amine group of Lys-19 for the first 41 ps of analysis, and the water that was coordinated to $O^{\delta 1}$ of Asp-73 for 35 ps in the middle of the analysis.

Another group of relatively immobile waters was the secondary hydration shell of the calcium ions. This consisted of water molecules with hydrogen atoms directed toward the calcium-binding sites. The cause of this unexpected behavior was the numerous carboxyl calcium ligands, which gave the calcium-binding sites a negative net charge in spite of the calcium ion. This led also the strange effect that one of the three sodium ions approached the EF calcium-binding site and remained there throughout.

Diffusion. The three-dimensional diffusion coefficient was obtained from the mean-square displacement as indicated by eq 5. It is enough to let Δt be large compared to the correlation

$$\lim_{\Delta t \to \infty} \langle [\mathrm{r}(t + \Delta t) - \mathrm{r}(t)]^2 \rangle = 6D\Delta t \qquad (5)$$

time (ζ^{-1}) of the velocity autocorrelation function if one calculates the diffusion coefficient from the slope of the mean-square displacement. For SPC water ζ^{-1} is less than one-tenth of a picosecond,[37] and thus it is enough to follow the water molecules for a few picoseconds. We calculated the mean-square displacements for water molecules with two different time spans, $\vartheta = 1.0$ and 20 ps. With $\vartheta = 20$ ps, we obtained straight lines for the mean-square displacement whereas, with $\vartheta = 1.0$ ps, the lines in some cases were curved even after 0.1–0.2 ps. Since the curvature differed between different layers, it is probably due to statistical uncertainty. The results are summarized in Figure 3, where one can see that the diffusion coefficient was larger in the inner layers than in the outer layers. In bulk, outside layer 14, it was approximately equal to what is obtained from bulk simulations (6.1×10^{-9} m^2/s).[33,38] With $\vartheta = 1.0$ ps, there was a maximum of the diffusion coefficient in layer 5 of about twice the bulk value whereas no such maximum could be seen with $\vartheta = 20$ ps. This is probably due to the fact that the water molecules diffused several angstroms in 20 ps, rendering observed diffusion coefficient an average over several layers. Wong and McCammon[24] found that the diffusion coefficient increased with distance from the protein whereas others have observed increased diffusion near a surface.[16,20] All these effects are, however, small compared to the retardation inferred from NMR results.[8]

Propagators and Radial Diffusion. To investigate the radial diffusion, it is useful to define the propagators $P_{ij}(\Delta t)$ (eq 6) where

$$P_{ij}(\Delta t) \equiv \langle P(j,t + \Delta t|i,t) \rangle_t = \langle N(j,t + \Delta t|i,t)/N(i,t) \rangle_t \qquad (6)$$

$P(j,t + \Delta t|i,t)$ is the probability that a molecule is in layer j at time $t + \Delta t$ given that it was in layer i at time t, $N(j,t + \Delta t|i,t)$ is the number of molecules in layer i at t and in layer j a time Δt later, $N(i,t)$ is the number of molecules in layer i at t, and $\langle ... \rangle_t$ implies a time average. We calculated the propagators $P_{jj}(\Delta t)$ for all 1-Å layers as well as all propagators $P_{ij}(\Delta t)$ for 5-Å layers. The propagators P_{jj} for 1-Å layers decay rapidly, and all of them except P_{22} reach their equilibrium values (the fraction of the total number of water molecules that layer j contains) within 10 ps.

The propagators P_{13} and P_{31} for the 5-Å-thick layers do not reach their equilibrium values, i.e. the fraction of water molecules in layers 3 and 1, respectively, during the whole simulation. This shows that the simulation is too short to give complete exchange of water between the different parts of the simulation cell.

A radial diffusion coefficient was estimated by fitting the simulated propagators to the corresponding quantity obtained from the solution of the macroscopic diffusion equation with proper boundary conditions. To avoid effects from waters coming from the same water layer in other boxes, we restricted the fitting to P_{22} through P_{55}. Carslaw and Jaeger[39] give the solution to the diffusion equation for a system outside an impenetrable sphere with radius b as eq 7 where $D_\perp$ is the radial diffusion coefficient,

$$C(r,t) = \frac{1}{8\pi r r' (\pi D_\perp t)^{1/2}} \left\{ \exp\left[-\frac{(r - r')^2}{4D_\perp t} \right] + \exp\left[-\frac{(r + r' - 2b)^2}{4D_\perp t} \right] - \frac{(4\pi D_\perp t)^{1/2}}{b} \exp\left[\frac{D_\perp t}{b^2} + \frac{r + r'}{b} - 2 \right] \times \mathrm{erfc}\left[\frac{(r + r' - 2b)}{2(D_\perp t)^{1/2}} + \frac{(D_\perp t)^{1/2}}{b} \right] \right\} \qquad (7)$$

C is the number concentration at r given there was a unit shell source at r' at $t = 0$, and erfc is the complementary error function. To get the corresponding propagator, we approximated each water layer by a 1-Å-thick spherical shell with radius of gyration equal

(37) This can be seen from the velocity correlation function of SPC water (Figure IV.5 in: Postma, J. P. M. "MD of H_2O, A Molecular Dynamics Study of Water". Ph.D. Thesis, Groningen, 1985) or inferred from the Einstein relation $D = kT/m\zeta$ (McQuarrie, D. A. *Statistical Mechanics*; Harper and Row: New York, 1976; p 455) and the diffusion coefficient.

(38) Teleman, O.; Ahlström, P. *J. Am. Chem. Soc.* **1986**, *108*, 4333.

(39) Carslaw, H. S.; Jaeger, J. C. *Conduction of Heat in Solids*; Clarendon: Oxford, England, 1959; eq [14.7(16)] with $h = 0$.

Table III. Radial Diffusion Coefficients As Obtained from Fitting the Propagators P_{jj} to Eq 7 and 8[a]

shell (class)	r_G/Å	$D_\perp$ (eq 7): b = 15.75 Å	$D_\perp$ (eq 7): b = 16.6 Å	$D_\perp$ (eq 8)	D_{total}	$D_\parallel$
2	16.25	3.7 ± 0.3		0.9 ± 0.3	9.7 ± 0.5	13 ± 1
3	17.15	6.2 ± 2.2		3.4 ± 0.0	10.5 ± 0.4	13 ± 1
4	18.65	9.1 ± 0.3	10.5 ± 0.7	8.5 ± 0.0	11.9 ± 0.4	13 ± 1
5	19.80	9.1 ± 0.1	9.3 ± 0.2	9.0 ± 0.0	12.5 ± 0.5	14 ± 1

[a] The errors are estimated from varying r_G in the interval given in Table II. For class 2 and eq 7, the thickness of the shell l was varied between 0.7 and 1 Å since the protein is assumed to be the inner wall of that shell. (b = 15.9 Å is obtained from r_G = 16.25 Å and the assumption that l = 0.7 Å for shell 2 whereas b = 16.6 Å gives the best fit for shell 4.) Also, the three-dimensional diffusion coefficient (cf. Figure 3) and $D_\parallel$ (cf. text) are given.

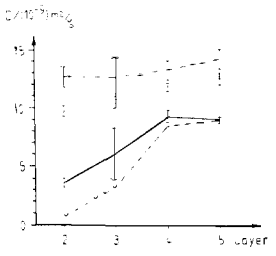

Figure 4. Radial diffusion coefficients for water molecules as function of layer obtained from fitting the propagators to eq 7 (solid curve) and to eq 8 (dashed curve). The errors were obtained according to the method described in Table III. For comparison, the diffusion coefficients obtained from the mean-square displacement (dotted) and the lateral diffusion coefficients from eq 9 (dot-dashed) are plotted.

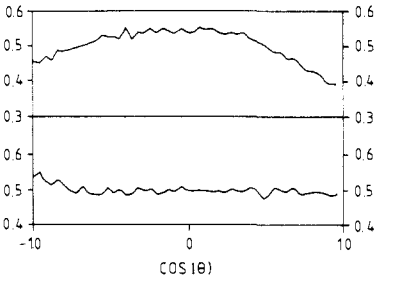

Figure 5. Distribution of cosine of the angle θ between radius vector and the dipole vector of the waters for layers 2 and 3 (upper curve) and 4 and 5 (lower curve). The curves show the probability density for finding a water molecule with a given value of cos θ.

to that of actual layer. Equation 7 was integrated numerically over r and r′ within the shell and divided by its volume (i.e. averaged over all **r**′ within the shell) to give the corresponding propagator. This was fitted to the simulated propagator in the interval 0–5 ps by varying $D_\perp$. For P_{22} the layer thickness was assumed to be smaller (0.7 Å) since the distance between waters and protein normally was more than 2.3 Å and b was set to the inner radius, i.e. 15.75 Å. For P_{44} and P_{55} the fit was made with two b values, 15.75 Å (as earlier) and 16.6 Å (which gives the best fit for P_{44}). The fitted diffusion coefficient changed about 15% on changing the b value in this way and was thus rather insensitive to the exact b value. To see if the impenetrable sphere influenced the diffusion coefficient, we also tried to fit the propagators from the simulation to free diffusion in a spherical coordinate system[40] (eq 8) where V_s is the volume of the layer

$$C(r,t) = \frac{1}{2r(\pi D_\perp t)^{1/2}} \int_{r_G-0.5l}^{r_G+0.5l} \frac{r'}{V_s} \left\{ \exp\left[-\frac{(r-r')^2}{4D_\perp t} \right] - \exp\left[-\frac{(r+r')^2}{4D_\perp t} \right] \right\} dr \quad (8)$$

investigated, l is the thickness of the layer, and the rest of the notation is as previously defined. The boundary condition at t = 0 was a uniform concentration ($1/V_s$) in the shell. Equation 8 was integrated numerically over r within the shell and fitted to the propagator in the interval 0–5 ps to obtain the diffusion coefficient $D_\perp$.

The result of both models is shown in Table III and is compared to the translational diffusion in Figure 4. The result in the two innermost layers is model dependent whereas the effect the impenetrable sphere has almost disappeared for P_{44} and outward. The diffusion coefficients obtained in this way essentially characterize the diffusion perpendicular to the protein surface. In layer 2 the radial diffusion coefficient is about one-fifth of the total diffusion coefficient D (obtained from the mean-square displacement)—$D_\perp \approx 2.1 \times 10^{-9}$ m²/s and $D \approx 9.5 \times 10^{-9}$ m²/s—but increases outward so that in layer 4 and 5 $D_\perp$ is about 75% of the total diffusion. The lateral diffusion coefficient $D_\parallel$ can be obtained from the total diffusion and the radial diffusion according to eq 9. The lateral diffusion coefficient for the layers 2–5 is given in Table III and Figure 4. In contrast to $D_\perp$, $D_\parallel$ is essentially constant over the entire interval and is about twice its bulk value (in the bulk $D_\parallel = D_\perp = D$).

$$D = (D_\perp + 2D_\parallel)/3 \quad (9)$$

Orientation of the Water Molecules. The orientation of water molecules was described by the angle θ between the dipole vector (defined as going from negative to positive) and the radius vector from the center of mass of the protein to the oxygen in the water molecule. The distribution of cos θ for 2-Å-thick layers is shown in Figure 5. In the innermost layer there was a preferential orientation of the dipole vector perpendicular to the radius vector. This agrees with several other studies[10,16-18] and is the expected orientation close to a body of low dielectric permittivity. The dipole vector was antiparallel to the radius vector more often than parallel. In the next 2-Å layer there seemed also to be a slight preference for the dipole vector to be antiparallel. This preference can be explained by the negative net charge of the protein, giving an average water polarization with positive charges toward the protein. The polarization effects on the water may be more pronounced than is obvious from Figure 5 as the spherical idealization of the protein made the analysis less sensitive.

Water Rotation. Reorientational autocorrelation functions for three perpendicular vectors in the water molecules have been calculated according to eq 10 where $\phi(t,\Delta t)$ is the angle between

$$C_j(\Delta t) = \langle P_j(\cos \phi(t,\Delta t)) \rangle_t \quad (10)$$

a vector at time t and the same vector Δt later, P_j is the Legendre polynomial of order j, and the brackets indicate a time average. The jth correlation time, τ_j, is defined through eq 11. Often the

$$\tau_j = \int_0^\infty C_j(t)\, dt \quad (11)$$

correlation function can be described as a sum of exponentials, i.e. eq 12 where the terms may represent different reorientation processes.

$$C_j(t) = A \exp(-t/\tau_{j1}) + B \exp(-t/\tau_{j2}) + C \exp(-t/\tau_{j3}) + \ldots \quad (12)$$

Figure 6a shows the logarithm of a time correlation function for the second Legendre polynomial of the dipole vector for waters in the innermost shell. After a short initial period the decay becomes approximately exponential with a time constant of about 1 ps. The correlation time for the second linear part, between

(40) Reference 39, eq [9.10(1)] with a = 0.

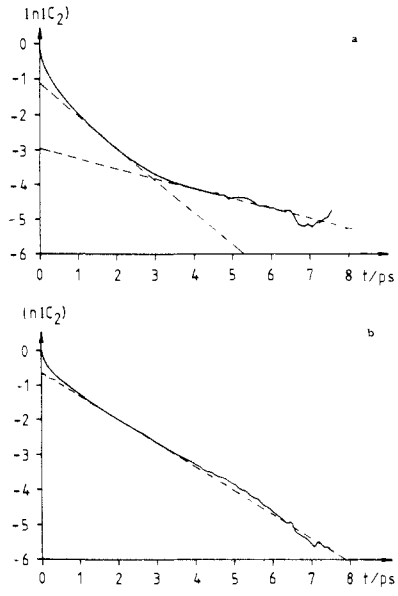

Figure 6. Logarithm of the correlation function for the second Legendre polynomial of the dipole vector for waters (a) in the innermost layer (2) and (b) for "bulk water" (layer 15). The analysis period (ϑ, see text) was 10 ps in both cases.

5 and 10 ps, is ≈4 ps. The numerical accuracy in the correlation function is about the same as the magnitude of the function after 10 ps (≈0.01). Hence, it is impossible to make any predictions about the longtime behavior, and we cannot preclude the existence of a third regime with a much longer correlation time. The same correlation function but for a water layer further away from the protein surface (Figure 6b) has only one linear part, with a correlation time of ≈1 ps. Thus, the second decay in Figure 6a is caused by the perturbation from the protein surface in terms of a restricted reorientational motion for the first water layer.

In order to characterize the reorientational behavior in different shells, we evaluated the correlation times τ_1 and τ_2 corresponding to first- and second-order Legendre polynomials. This was done in two different ways. First, we made a fit of the correlation function to a single exponential in the interval 0.5–2 ps; second, we evaluated the integral (eq 11) directly. Since the water molecules were followed for a rather short interval, we had to approximate the tail of the correlation function with a single exponential for times larger than ϑ when evaluating the integral. The results for two different analysis periods (ϑ = 3 and 10 ps) are shown in Figure 7. First, we note that the τ_2 values did not differ very much between the two analysis periods ϑ used as the correlation function was almost zero within a few picoseconds. Second, the correlation times as calculated from the integrals were always shorter than the ones obtained from the fitting. This was a result of the initial librational decay of the correlation functions. Third, we note that the layer dependence again becomes less pronounced on increasing the analysis period.

The dependence of the correlation times on the distance to the protein is unexpected. Experimental results seem to indicate that reorientation slowed down near the protein surface with increased correlation times. Here, we report a partially opposite result, namely a steady increase in the correlation times from layer 4 to layer 15. In simulations of pure water[33] and water in an EDTA solution[38] the correlation times were about the same as for layer 4, i.e. our minimum correlation times.

Conclusion

In this study the dynamical behavior of water is only weakly influenced by the protein molecule. A few water molecules are immobilized at the protein surface for a short while, and the radial diffusion is reduced near the protein surface. On the other hand, lateral diffusion and rotation are somewhat faster a few angstroms from the protein surface than in the bulk. These results disagree strongly with the widespread notion that water molecules at surfaces are immobile, having completely different dynamical behavior compared to bulk. They also differ, to a lesser extent, from NMR relaxation data, usually interpreted as implying that the local reorientational motion is significantly slower than in bulk. At present, we are unable to resolve this latter discrepancy. One possible explanation could be the somewhat arbitrary potential functions used in the simulation or the truncation of interactions necessary to make the simulation feasible. However, a wide range of different simulations report findings similar to ours and, taken together, throw some doubt on the interpretation of experimental relaxation results. NMR relaxation studies indicate a long time tail in the reorientational correlation function. This long time tail is not accessible to MD simulations, but we conclude that its origin is not due to slow interfacial diffusion of water molecules.

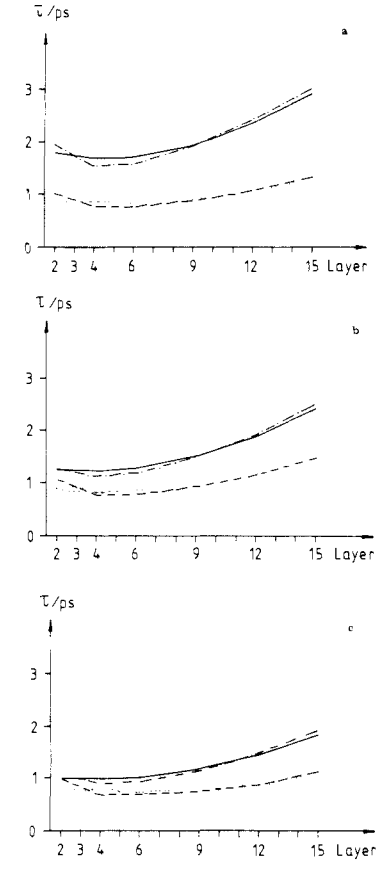

Figure 7. Correlation times for three vectors in water molecules as a function of the starting layer: (a) the dipole vector, (b) the vector in the molecule plane perpendicular to the dipole vector, and (c) the vector perpendicular to the molecular plane. All values were obtained by fitting the correlation function to an exponential in the interval 0.5–2.0 ps: solid curve, τ_1 with analysis period ϑ = 10 ps; dot-dashed curve, τ_1 with ϑ = 3 ps; dotted curve, τ_2 with ϑ = 10 ps; dashed curve, τ_2 with ϑ = 3 ps.

Acknowledgment. We thank Dr. Bertil Halle for valuable discussion. We also thank IBM Corp. for generous allocation of computer time on the IBM 3090-150 VF installed at Lund. P.A. acknowledges a grant from the Swedish Sciences Research Council.

Registry No. H_2O, 7732-18-5.